COMPARATIVE STUDY AND OPTIMIZATION OF SPECIAL-SHAPED METAL SEALING RINGS WITH SURFACE IMPERFECTIONS FOR MANDREL CASING HANGERS

Yaoming Zhang[1,2,3,4], Xuliang Zhang[1,2,3,4], Fudong Liu[5], Pengcheng Wang[1,2,3,4], Jianfei Wang[5,], Fei Zhan[5], Rui Ma[5]*
[1]CNPC R & D Center for Ultra-Deep Complex Reservior Exploration and Development, Korla, Xinjiang, 841001, China;
[2]Engineering Research Center for Ultra-Deep Complex Reservoir Exploration and Development, Korla, Xinjiang, 841001, China;
[3]Xinjiang Key Laboratory of Ultra-Deep Oil and Gas, Korla, Xinjiang, 841001, China;
[4]PetroChina Tarim Oilfield Company,Korla, Xinjiang, 841001, China;
[5]CNPC Bohai Equipment Manufacturing Co., Ltd.,Tianjin 300457, China

Abstract - In order to deeply analyze the influence of surface defects on the strength and perfection of sealing rings of the hanger, this paper conducts a comparative calculation of the sealing material and surface contact pressure based on the sealing specific pressure principle. Given the variation laws of the surface contact width and contact pressure of the sealing rings under different pressures, working models of different special-shaped metal sealing rings are established based on the finite element method. Compare and analyze the variation laws of sealing contact pressure and material matrix stress of different sealing rings. Finally, the strength and sealing performance of different special-shaped metal sealing rings are compared based on multiple regression analysis. The results show that the mechanical properties and contact pressure of X-shaped and straight U-shaped metal sealing rings fluctuate greatly, their contact widths are relatively small when there are defects. For imperfect sealing rings, the mechanical properties and sealing performance of ball-drum metal sealing rings and elliptical U-shaped sealing rings are relatively stable, and their contact widths are relatively large. The imperfect sealing ring reduces the strength of the metal material. The performance improvement of the linear U-shaped and X-shaped sealing rings during the optimization process is relatively small. This indicates that their structural forms have a relatively weak response to parameter changes. The optimized U-shaped metal sealing ring ensures good adhesion at the sealing interface and load-bearing capacity. Meanwhile, the minimum equivalent stress is all controlled below 290 MPa, which is conducive to reducing the failure risk caused by local high stress fields, and improving the fatigue life and long-term service reliability of the structure.

Keywords: Casing hanger, Sealing ring, Imperfection, Strength, Stress, Multiple regression analysis.

1. Introduction

With the increase in production and wellhead pressure, the safety of the casing head of high-temperature and high-pressure gas wells is related to the integrity of the well. The damage to the integrity leads to the destruction of the cement ring structure of the casing, resulting in wellhead uplift or wellhead leakage accidents [1-3]. At present, the demand for casing hangers with a pressure of over 140MPa at the wellhead is gradually increasing. Experts and scholars have conducted some related research on casing hangers for ultra-high pressure wellheads. Yingying Wang et al. utilize the structural axial symmetry characteristics of the C-shaped metal sealing ring, decomposed it into the cantilever beam model and the simply supported beam model for theoretical analysis [4]. Zhi Zhang et al. analyze the failure causes of the Cava hanger by using optical microscopy, scanning electron microscopy, energy dispersive spectrometer and other techniques. The research results mainly prove that the Cava hanger cannot adapt to the ultra-high pressure operating conditions [5-8]. Liu Yang et al. conducted a systematic study on the metal sealing ring of the gas well wellhead under 140MPa high pressure and

© 2026. The Author(s). Published by Cefin Publishing House – Bucharest, https://ijomam.com/

Copyright: © 2026 by the authors. Licensee IJOMAM, Romania. This article is an open access article distributed under the terms and conditions of the Creative Commons. Attribution (CC BY) license (https://creativecommons.org/licenses/by/4.0/)
dx.doi.org/10.17683/ijomam/issue24.14

extreme temperature by using a fully metal-sealed hanger device[9-11]. Janardhan Rao Saithala et al. studied high-pressure/high-temperature sulfur-containing gas well tubing hangers. The microstructure study analyzed by optical and scanning electron microscopy (SEM) revealed several harmful metallurgical phases[12]. Yong Chen et al. introduced the structure and working principle of the φ 273.1mm casing hanger device, derived the mechanical balance equation of the main seal and the casing head step, analyzed the sealing performance of the casing hanger device[13]. Jing Zeng et al. discussed the lateral load-bearing stability of conventional wellhead devices and suction anchor wellhead devices under the influence of wellhead loads [14,15]. Harshkumar Patel et al. proposed a finite element modeling method to evaluate the performance and applicability of conventional elastomer hanger sealing components. For this purpose, a three-dimensional computer model composed of liner, casing and sealing assembly elements is used to evaluate the sealing performance based on the contact stress generated at the interface of the sealing tube [16-18]. Pablo Cirimello et al. studied the failure problem of a 5 "casing hanger in an oil well. The analysis found that the combined load of internal pressure, casing weight and tightening torque caused the structural stress of the hanger to approach the yield strength of the material[19,20].

The above literature has studied the limitations of conventional slip hangers and conducted in-depth research on the sealing ring of mandrel hangers. It has proposed various types of metal sealing rings and verified the rationality of metal sealing rings. This paper mainly draws on the research results of predecessors and aims to conduct in-depth research on the existing four commonly used sealing rings under various complex working conditions. The existing literature has not yet conducted relevant research on whether the sealing effect of metal seals and sealing parts meets the actual requirements when there are defects. In fact, similar working conditions are more likely to occur at the four-way wellhead. During transportation, movement and installation, the sealing parts often get knocked and collided. The surface accuracy of the mandrel, four-way and sealing parts is not as accurate as the factory surface. Especially the metal sealing contact surface needs further verification of its sealing performance. Therefore, it is necessary to conduct a systematic analysis of the sealing parts with surface defects. In order to obtain analysis results that are consistent with the actual working conditions. Provide theoretical guidance for the actual service assessment of the four-over-wellhead mandrel type oil casing hanger.

2. Materials and Methods

As shown in Figure 1, the existing mandrel-type casing hanger is usually composed of a combination of rubber and metal to form the main sealing unit. The operators have not taken effective protective measures for the installation of the mandrel-type casing hanger. During the transportation and installation process, the surface of the metal sealing ring will be damaged, forming defects, which will have a certain impact on the sealing performance. This article will conduct research on the sealing performance of defective seals.

Figure 1: The sealing ring before and after use

The seal between the sealing ring of the mandrel-type casing hanger and the body is a contact seal between the metal surfaces. Generally, if the fluid leaks, it will persist. The flow resistance of the fluid when passing through a tiny gap can be expressed by Equation (1) as:

$$\Delta R \propto \Delta L / S \qquad (1)$$

In the formula, △R represents the flow resistance, N; △L-Minimum length, mm; S-Cross-sectional area, mm ^{2}.

From Equation (1), it shows that increasing △L and decreasing S can increase the resistance to fluid flow. Figure 2 shows the contact process between the metal sealing surfaces. During the contact process, the cross-sectional area S gradually decreases, the leakage resistance △R gradually increases, and finally an effective seal is formed.

(a) Initial contact stage (b) After sealing

Figure 2: Microscopic process of metal-metal sealing

From the perspective of gas sealing contact energy, as shown in Figure 3, the longer the contact surface, the lower the contact pressure gradually. A large contact pressure can be achieved within 0-4mm, and thus sealing can be realized.

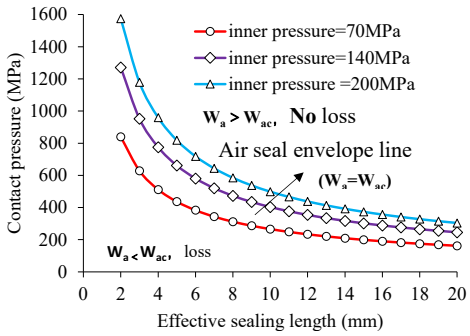

Figure 3: Variation curves between the average contact pressure and the effective sealing length of the sealing surface

3. Results and Discussions

3.1 Analysis of the Ball-drum Sealing Ring

According to the overall structural dimensions of the mandrel-type casing hanger shown in Figure 4. According to references [4,9], the core shaft material is high-temperature nickel-based alloy material, with a yield strength of approximately 750MPa and a tensile strength of approximately 985MPa.The elastic modulus of the mandrel, four-way and metal seal is 2.06×105MPa, and the Poisson's ratio is 0.3.

As shown in Figure 4, the sealing unit of the casing hanger mainly adopts a ball drum metal sealing ring. In order to verify the stress-strain law and sealing performance of the metal sealing ring under different loads, the lower end face of the four-way is fixed in Figure 4, and tensile loads F=50t-400t were respectively applied to the lower end face of the mandrel. Figure 5 shows the finite element calculation model of the metal seal under load.

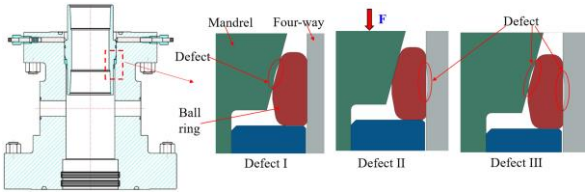

Figure 4: Assembly drawing of the sealing ring

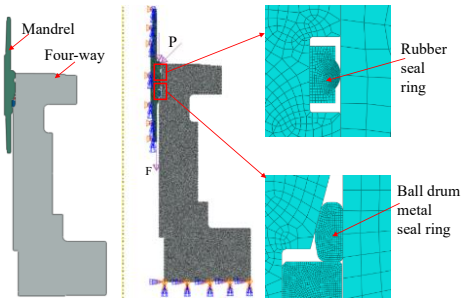

(a) Assembly model (b) Finite element model

Figure 5: Assembly drawing and finite element model of the sealing ring

As shown in Figure 6(a)-(c), a stress concentration area forms at the defect location as the load increases when the tensile load F is within the range of 50 tons to 400 tons, similar to Hertz stress, fluctuating within the stress range of 314.7 MPa to 326.6MPa. Figure 6(d) shows that the seal fluctuates within the stress range of 128.1 MPa to 307.5MPa. The maximum stress of the ball-drum type sealing ring mainly occurs in the middle and upper parts. The upper part can undergo plastic deformation, and the stress at the contact part with the support ring is relatively small. The support ring can effectively reduce the overall stress of the ball-drum type metal sealing ring. In comparison, when there are defects in the sealing system, the overall stress of the sealing parts is relatively small, but the strength of the contact parts exceeds the yield limit. However, when there are no defects, the overall deformation of the sealing parts is relatively small, and there is no stress concentration phenomenon, which is conducive to extending the service life. The maximum stress of each key component did not exceed the corresponding material yield strength. This sealing system meets the load-bearing conditions.

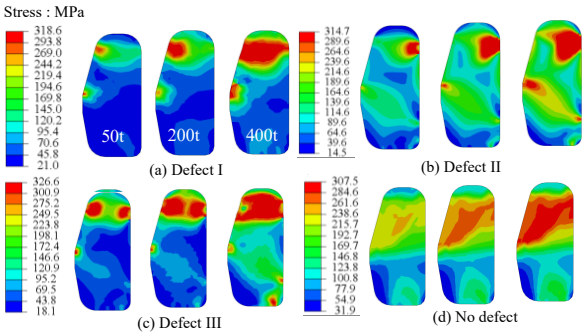

Figure 6: Stress contour of ball drum sealing rings

Figure 7 and Figure 8 show the contact pressure law curves of sealing rings with different defects. Under the three defect states, the contact pressure of each sealing ring varies between 100 and 200MPa. The maximum contact pressure of defect III is greater than that of the other two defects, and the curve laws are approximately the same. The contact pressure varies between 300 and 400MPa when there are no defects. The absence of defects can improve the sealing performance of the ball-drum type sealing ring. When there are no defects, the contact path of the sealing ring is relatively wide. Although the contact pressure of the defective seal can meet certain sealing requirements, the contact width is still relatively small, which is not conducive to long-term sealing.

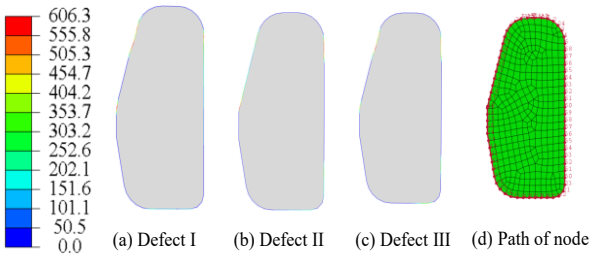

Figure 7: Contact path of the ball drum sealing ring

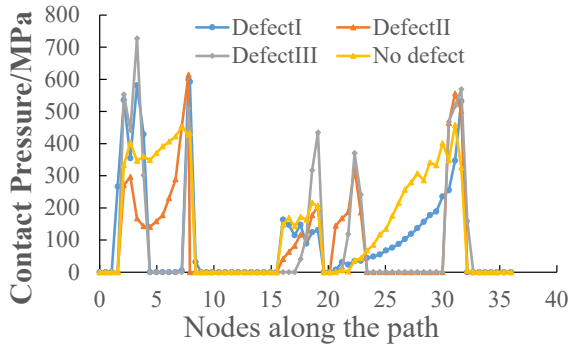

Figure 8: Contact pressure of the ball drum ring

3.2 Analysis of Linear U-shaped and X-Shaped Metal Seals

Figure 9 shows a combination of linear U-shaped and X-shaped metal sealing rings. This structure is commonly used in the sealing units of casing hangers, and the material of the metal sealing unit is the same as the aforementioned material. In the analysis, the load and boundary conditions were similar to those in the previous analysis. Tensile loads F=100t-400t were respectively applied to the lower end face of the mandrel, and pressure loads P=50MPa-140MPa were respectively applied to the upper end face of the sealing pressure ring.

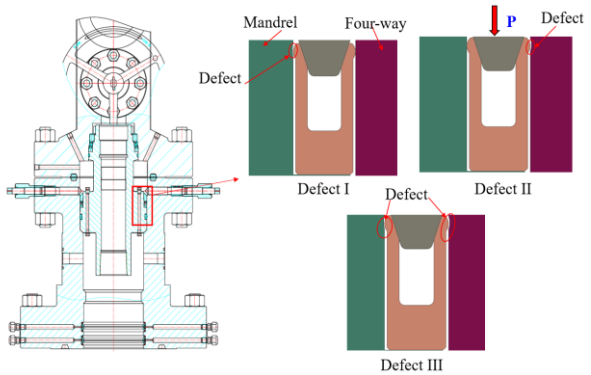

Figure 9: Assembly drawing of the sealed structure

As shown in Figure 10, the stress change of the lower linear U-shaped sealing ring is relatively stable with the increase of load, while the stress of the upper X-shaped metal sealing ring rises significantly, and its deformation gradually intensifies with the increase of pressure.

Especially the maximum stress endured by the X-type metal sealing ring is between 274 MPa and 322 MPa when the upper load reaches 120MPa to 140MPa. Due to the compression effect, the X-type metal sealing ring undergoes significant deformation, and the overall stress level gradually increases with the height direction. Although it has enhanced the sealing effect to a certain extent, its deformation degree has approached or even exceeded the load-bearing limit of the material, posing a potential risk of structural failure. Therefore, although this sealing ring can still achieve effective sealing under high load conditions, from the perspective of material mechanical properties, an in-depth assessment of its long-term service reliability is required.

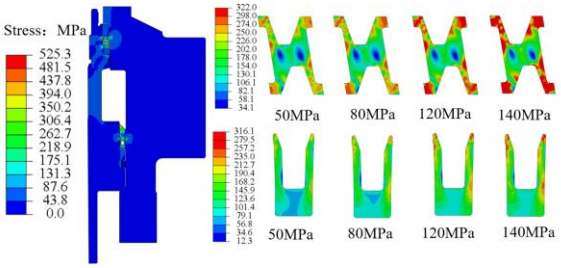

Figure 10: Stress contour of the metal sealing ring

As shown in Figure 11(a)-(c), a stress concentration area forms at the defect location as the load increases when the compressive load P is within the range of 50MPa to 140MPa tons, similar to Hertz stress, fluctuating within the stress range of 319MPa to 328.8MPa. The overall stress of the defective linear U-shaped metal sealing ring is relatively large, and the force is extremely uneven. The right half of the part undergoes significant plastic deformation, while the left half does not. The support ring can effectively reduce the overall stress of the ball drum type metal sealing ring. In comparison, the overall stress of the linear U-shaped metal sealing ring is relatively small within the range of 50MPa to 140MPa when there are no defects in Figure 11(d). The maximum stress at the contact parts with the core shaft and the four-way is 316.1MPa when the pressure is 140MPa, and the stress at other parts is much less than the yield stress value. The maximum stress of the seal is 316.1MPa. The overall force on the seal is very uniform with minimal deformation, no stress concentration, and no obvious plastic deformation, which is conducive to extending the overall service life.

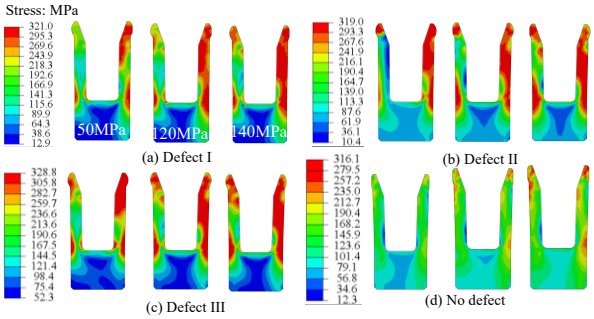

Figure 11: Stress contour of linear U-shaped rings

Figure 12 shows the contact path diagram of the sealing ring, and Figure 13 shows the contact pressure curve of the linear U-shaped metal sealing ring. The peak contact pressure of the four sealing rings ranges from 300MPa to 600MPa. The contact pressure curves of different structures are consistent in pattern, and the sealing pressure is relatively stable. Therefore, the contact pressure of the linear U-shaped metal sealing ring fluctuates greatly, and the contact width of various structures is relatively small, which is not conducive to the stability of the seal.

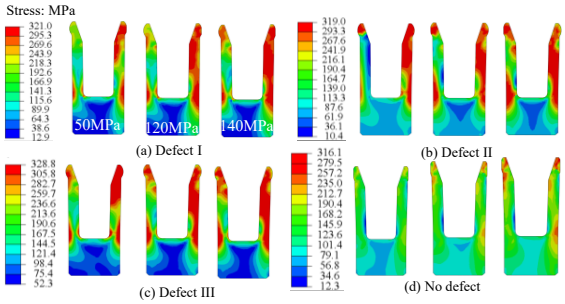

Figure 12: Contact paths for metal sealing rings

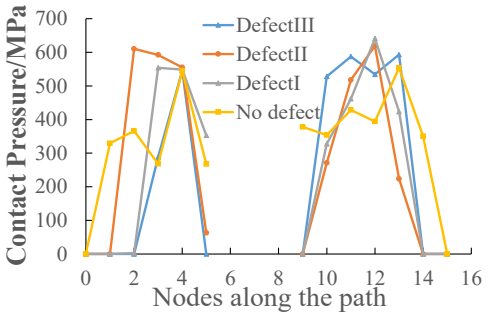

Figure 13: Contact pressure curves with different defects

3.3 Analysis of Elliptical U-shaped Metal Sealing Ring

The materials of the mandrel, four-way and sealing parts are the same as mentioned above. Tensile loads F=50t-400t are respectively applied to the lower end face of the mandrel, and pressure loads P=50MPa-140MPa are respectively applied to the upper end face of the sealing pressure ring, as shown in Figure 14.

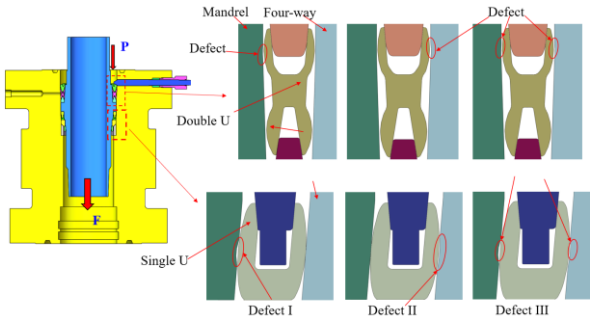

Figure 14: Assembly drawing of U-shaped structure

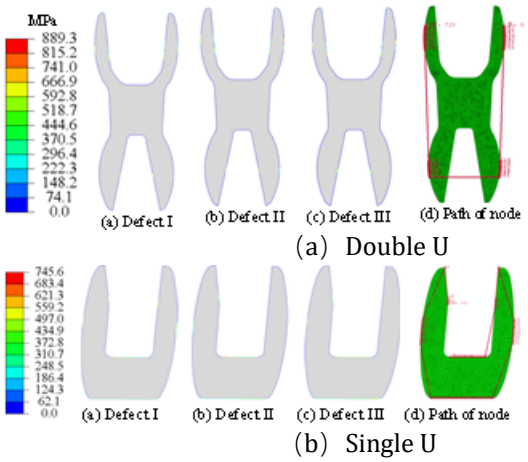

Figure 15: Contact paths for metal sealing rings

Figure 15 shows the contact paths for metal sealing rings. Figure 16 (a) shows the contact pressure curve of the double U-shaped metal sealing ring. When there is a defect, the peak contact pressure between the left side and the core shaft and the four-way contact part is between 400MPa and 780MPa, and the peak contact pressure between the right side and the four-way contact part is between 300MPa and 820MPa. When there are no defects, the peak contact pressure ranges from 300MPa to 780MPa, and the contact width is basically the same. In Figure 16(b), the contact pressure curve of the single U-shaped metal sealing ring shows that when there is a defect, the peak contact pressure at the left contact part with the core shaft is between 200MPa and 700MPa, and the peak contact pressure at the right contact part with the four-way seal is between 300MPa and 700MPa. When there are no defects, the peak contact pressure ranges from 400MPa to 750MPa, and the contact widths with and without defects are basically the same. Therefore, relatively speaking, the contact pressure fluctuation of the double U-shaped metal sealing ring is small, and it can effectively seal a gas pressure of 140MPa, which is conducive to the stability of the seal.

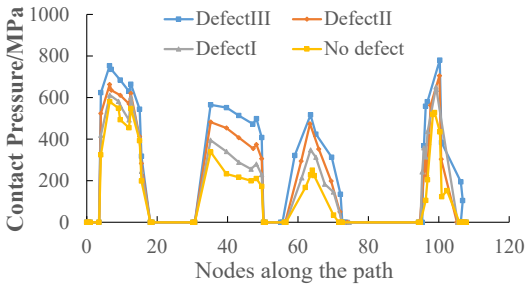

(a) Double U

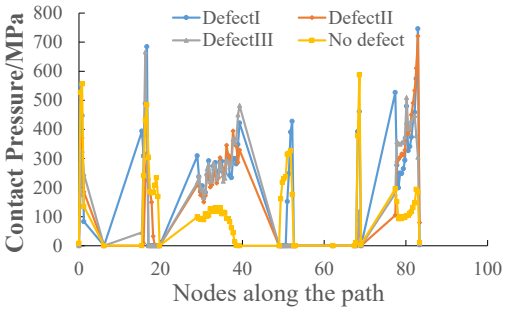

(b) Single U

Figure 16: Contact pressure curves of sealing rings

Through finite element calculation, it is found that among the four types of special-shaped metal seals, the mechanical properties and contact pressure of X-shaped and linear U-shaped metal seals fluctuate greatly, and their contact widths are relatively small. The mechanical properties and sealing performance of ball-drum type metal seals and elliptical U-shaped seals are relatively stable, and their contact widths are relatively large.

3.4 Research on Optimization of Sealing Ring of Mandrel Hanger

The aforementioned main research focuses on the stress-strain laws of different metal sealing rings under load conditions. To analyze the influence of different metal sealing ring parameters on sealing performance, a comparative study is conducted on the parameters of four special-shaped metal structures. The key dimensions and parameters of each structure are shown in Figure 17. The key parameters of the four types of special-shaped metal structures mainly include the size and shape of the contact surface and the yield strength of the sealing parts. These parameters determine the values of contact pressure and stress. Based on the analysis of the key parameters of the four types of special-shaped metal structures, the influence degree of the response factors acting together on the sealing effect of the casing hanger is obtained, providing a theoretical reference basis for the design and manufacture of the casing hanger.

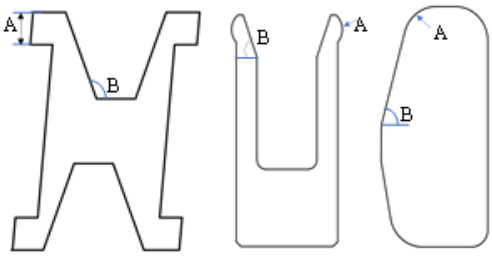

(a) X-shaped (b) linear U (c) Ball-drum

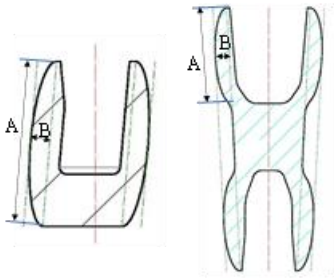

(d) Single U (e) Double U

Figure 17: Five types of special-shaped metal seal

In Figure 17 (a), A represents the original width of the contact surface (A=2.5-4.5mm), and B is the included Angle of the pressure ring (B=100° - 120°). In Figure 17 (b), A represents the radius (A=1.5-3.5mm), and B represents the contact inclination Angle (B=60°-80°). In Figure 17 (c), A represents the original width of the contact surface (A=2.5-4.5mm), and B represents the Angle between the pressure rings (B=68°-80°). In Figure 7 (d), A represents the length of the major axis of the ellipse (A=18.5-23.5mm), and B represents the length of the minor axis of the ellipse (B=3.5-4.5mm). In Figure 17(e), A represents the length of the major axis of the ellipse (A=18.5-21.5mm), and B represents the length of the minor axis of the ellipse (B=3.8-4.8mm). The yield strength range of each metal seal is C (C=270-350MPa).

Cp,σ-The optimization objective functions of the key parameters of the four types of special-shaped metal structures are:

$$\begin{cases} Max[Cp] \\ Min[\sigma] \end{cases} \tag{2}$$

In the formula: Cp represents the maximum contact pressure, MPa. σ is the minimum von Mises stress, MPa. According to the mutual influence law of the key structural parameters of each sealing part, the response surface diagram of the maximum contact pressure and the minimum von Mises stress is obtained, as shown in Figure 18.

It shows that the contact pressure variation trend of the single U-shaped sealing ring under different structural parameters in Figure 18(a). Specifically, the contact pressure between the sealing ring and the sealing surface shows a slow downward trend as the influencing factors A (long wheelbase distance)

and B (short wheelbase distance) gradually increase, indicating that the increase in structural dimensions weakens the tightness of the sealing interface to a certain extent. The influence of the variation in the yield strength of the material on the contact pressure exhibits more complex nonlinear characteristics: in the initial stage, as the yield strength increases, the rigidity of the material intensifies, resulting in a decrease in its elastic deformation capacity during assembly, thereby reducing the contact pressure. However, the material's ability to resist plastic deformation significantly improves, and thus the contact pressure rises accordingly when the yield strength further increases by 315.4MPa.

Within the range of parameters studied, the maximum contact pressure generated by the sealing ring at the sealing interface can reach 512.6MPa when the long wheelbase distance is 20.56mm and the short wheelbase distance is 3.94mm. This value not only reflects the optimal performance of the sealing under this combination of structural parameters, but also provides an important theoretical basis and engineering reference for the subsequent optimization of sealing design and improvement of sealing reliability. It shows that the minimum stress on the outside of the sealing ring first decreases and then increases with the increase of the long wheelbase distance in Figure 18(b), and slowly decreases with the increase of the short wheelbase distance.

Although the material parameters have a relatively small impact on the equivalent effect force changes, from the perspective of overall sealing performance, appropriately increasing the yield limit can help improve the adhesion and adaptability of the sealing interface, thereby enhancing the sealing effect. If the long wheelbase distance is too large, it will cause the contact pressure distribution to be overly dispersed, reducing the sealing reliability. Therefore, in the optimization design, the matching relationship of the three structural parameters needs to be comprehensively considered to achieve the best sealing performance.

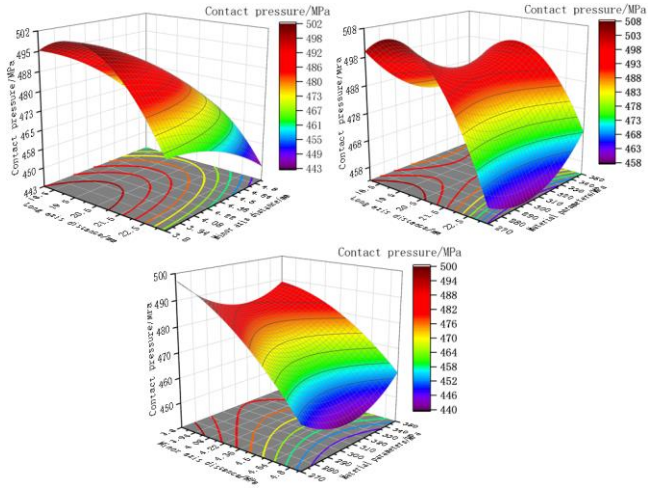

(a) Response surface of contact pressure

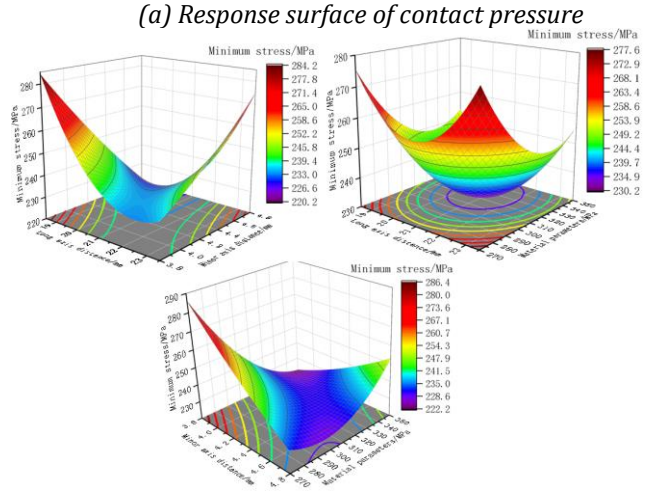

(b) Response surface of minimum stress

Figure 18: Response surface of the objective function and the design variable of the single U

As shown in Figure 19 (a), the performance of the double U-shaped metal sealing ring is obvious. Its contact pressure drops sharply at first and then rises slowly when the long wheelbase distance increases. Its contact pressure decreases slowly when the short wheelbase distance increases. However, the influence of material parameters on contact pressure is relatively small.

As shown in Figure 19 (b), there is a significant compound relationship in the influence of the three factors on the contact pressure. With the increase of the long wheelbase and the short wheelbase, the minimum contact pressure first decreases and then increases. Its equivalent stress reaches the lowest value when the long wheelbase is 19.86mm and the short wheelbase is 4.15mm.

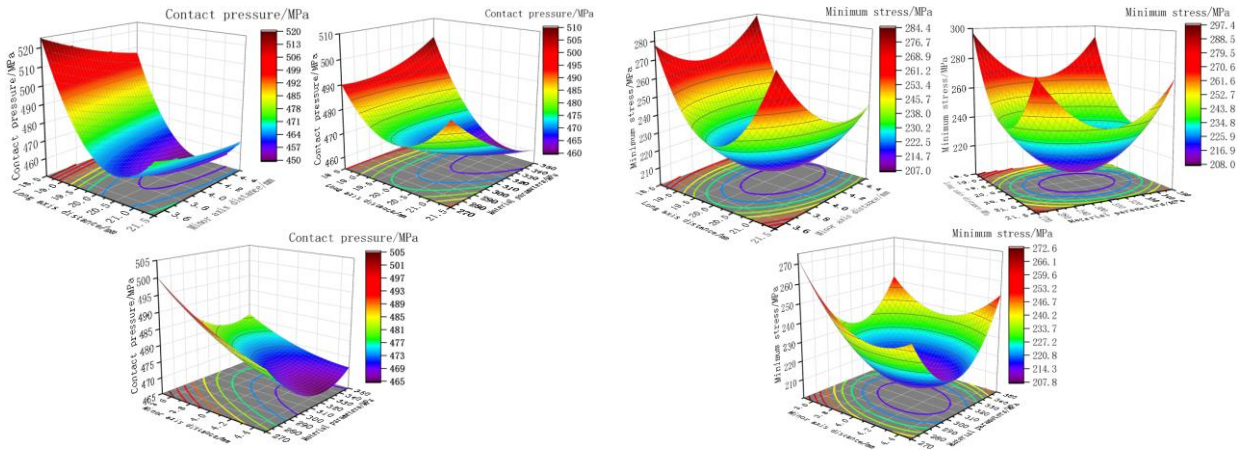

(a) Response surface of contact pressure *(b) Response surface of minimum stress*

Figure 19: Response surface of the objective function and the design variable of the double U

As shown in Figure 20(a), the maximum contact pressure on the response surface of the ball drum metal seal is approximately 480MPa, and the minimum equal force is approximately 285.7MPa.

As the radius of the ball drum increases, the contact pressure first increases and then gradually decreases. Under the influence of three response factors, the contact pressure gauge shows a nonlinear relationship. As shown in Figure 20(b), with the increase of radius, the minimum stress gradually decreases. The minimum stress reaches a minimum of 294.6MPa when the radius is 3.2mm and the contact inclination angle is 78°.

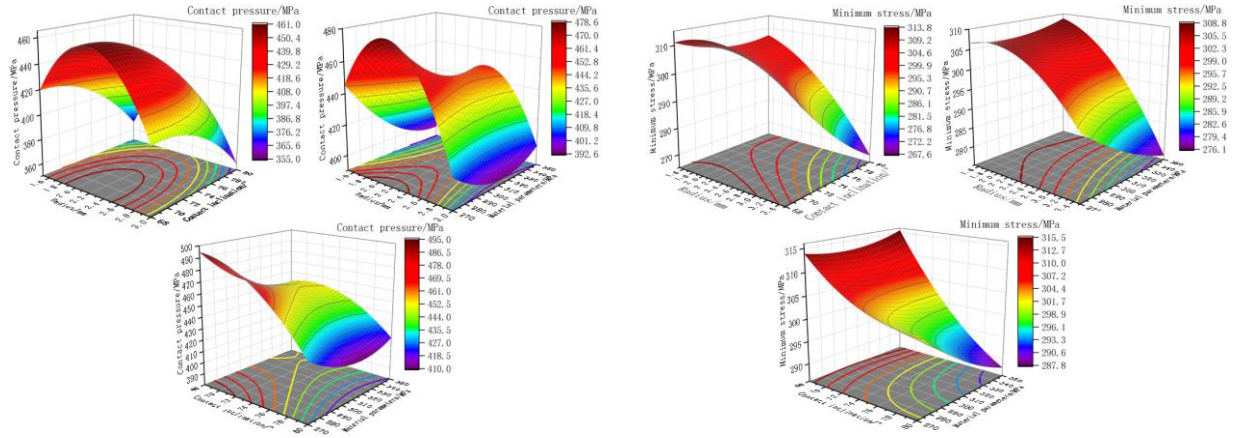

(a) Response surface of contact pressure *(b) Response surface of minimum stress*

Figure 20: Response surface of the objective function and the design variable of the ball drum

Binary regression analysis is conducted using response surface curves, with max [Cp] and min [σ] as the targets. After parameter optimization, the comparison results are shown in Table1.

Table.1 Comparative analysis of optimization results

Target	Struct-ure	Before opti /MPa	After opti /MPa	Error	Optimi rate
[Cp]	Str-U	569	502	2.5%	11.6%
	D-U	584	511	1.8%	12.6%
	Ball	524	478	3.6%	8.6%
	Sin- U	518	480	3.0%	7.3%
	X	495	468	2.7%	5.5%
[σ]	Str-U	297	265	4.7%	10.6%
	D-U	329	287	3.5%	12.8%
	Ball	338	306	3.7%	9.6%
	Sin-U	351	322	4.1%	8.2%
	X	350	334	3.9%	4.8%

As shown in the research results of Table 1, the performance differences of single U-shaped and double U-shaped sealing rings before and after optimization are the most significant among the five metal sealing ring forms analyzed, demonstrating strong optimization and structural response potential. In contrast, the optimization effect of the ball-drum type sealing ring is moderate, while the optimization effect of the linear U-shaped and X-shaped sealing rings is relatively weak, indicating that they are less sensitive to changes in design parameters. Specifically, for the single U-shaped metal sealing ring, after optimization, the optimization rates of its maximum contact pressure (max [Cp]) and minimum equivalent stress (min [σ]) reached 11.6% and 10.6% respectively. This indicates that by adjusting the structural parameters, the pressure distribution characteristics of its sealing interface can be effectively enhanced, and the stress concentration phenomenon can be improved, thereby strengthening its sealing performance and structural stability. For the double U-shaped sealing ring, due to the symmetry of its geometric configuration and the dual sealing mechanism, the optimization effect is more significant. The optimization rates of its maximum contact pressure and minimum equivalent stress both exceed 12%, demonstrating superior mechanical response characteristics and higher structural reliability

The ball drum sealing ring also demonstrated a certain performance improvement ability during the optimization process. The optimization rates of its maximum contact pressure and minimum equivalent stress were 8.6% and 9.6% respectively. Although the optimization extent is not as large as that of single U-shaped and double U-shaped structures, it still shows certain engineering application value. In contrast, the performance improvement of the linear U-shaped and X-shaped sealing rings during the optimization process is relatively limited, and the optimization effect is not obvious. This indicates that their structural forms may have approached the performance limit within the current design parameter range or have a weak response to parameter changes

The optimized single U-shaped and double U-shaped metal sealing rings stand out particularly in key performance indicators: their maximum contact pressures both exceed 500 MPa, ensuring good adhesion and load-bearing capacity at the sealing interface. Meanwhile, the minimum equivalent stress is all controlled below 290 MPa, which is conducive to reducing the failure risk brought by local high-stress areas and improving the fatigue life and long-term service reliability of the structure. Therefore, taking into account the optimization potential and the final performance indicators comprehensively, the single U-shaped and double U-shaped metal sealing rings demonstrate superior sealing performance and engineering applicability among the five structural forms.

Furthermore, the errors generated during the optimization process were all controlled within an acceptable range and were basically consistent with the error analysis results conducted by the Design-Expert software, verifying the reliability and applicability of the optimization model. The results show that the adopted optimization method can effectively improve the key performance indicators of the sealing ring and has good engineering application value.

4. Conclusions

Through simulation optimization research, the following conclusions have been drawn:

(1) Among the four types of special-shaped metal seals, the mechanical properties and contact pressure of X-shaped and linear U-shaped metal seals fluctuate greatly, and their contact widths are relatively small when there are defects. For incomplete sealing rings, the mechanical properties

and sealing performance of ball-drum metal seals and elliptical U-shaped seals are relatively stable, and their contact widths are relatively large.

(2) The incompleteness of the sealing ring reduces the strength of metal materials. For metal seals, defect incompleteness has a relatively small impact on contact width and contact pressure.

(3) For the single U-shaped metal sealing ring, the optimization rates of its maximum contact pressure and minimum equivalent stress reached 11.6% and 10.6% respectively after optimization. This indicates that the pressure distribution characteristics of its sealing interface can be effectively enhanced by adjusting the structural parameters, and the stress concentration phenomenon can be improved, thereby strengthening its sealing performance and structural stability. For the double U-shaped sealing ring, due to the symmetry of its geometric configuration and the dual sealing mechanism, the optimization effect is more significant. The optimization rates of its maximum contact pressure and minimum equivalent stress both exceed 12%, demonstrating superior mechanical response characteristics and higher structural reliability.

(4) The ball drum sealing ring also demonstrated a certain performance improvement capability during the optimization process. The optimization rates of its maximum contact pressure and minimum equivalent stress were 8.6% and 9.6% respectively.

(5) The optimized single U-shaped and double U-shaped metal sealing rings stand out particularly in key performance indicators: their maximum contact pressures both exceed 500 MPa, ensuring good adhesion and load-bearing capacity at the sealing interface. Meanwhile, the minimum equivalent stress is all controlled below 290 MPa, which is conducive to reducing the failure risk brought by local high-stress areas and improving the fatigue life and long-term service reliability of the structure.

Acknowledgement

The authors are grateful for the financial support from research and development of ultra-high pressure wellhead and supporting equipment (2015ZG15) of Major Science and Technology Project of China National Petroleum Corporation.

References

[1] Mark J. Kaiser (2017). Rigless well abandonment remediation in the shallow water U.S. Gulf of Mexico[J]. Journal of Petroleum Science and Engineering,151,94–115. http://dx.doi.org/10.1016/j.petrol.2017.01.004.

[2] Lian,W., Li,J ., Xu,D.R.,Lu, Z.Y., Ren,K., Wang,X.G., Chen, S. (2023). Sealing failure mechanism and control method for cement sheath in HPHT gas wells[J]. Energy Reports, 9 ,3593–3603. https://doi.org/10.1016/j.egyr.2023.02.048

[3] Moses,J. B. K., Oludolapo, A.O. (2022). Geothermal wellhead technology power plants in grid electricity generation: A review[J]. Energy Strategy Reviews,39,100735. https://doi.org/10.1016/j.esr.2021.100735.3860.

[4] Wang,Y.Y., Luo, W.T., Liu,S.J., Feng, H.Z., Li J.C., Wang,J.J. (2022). A model for reliability assessment of sealing performance of the C-shaped metal sealing ring at the outlet of the subsea tubing hanger[J]. Ocean Engineering, 243,110311.https://doi.org/10.1016/j.oceaneng. 2021.110311.

[5] Zhang Z., Sang,P.F., Sang,Z.P., Hou,D., Lv,Y.Y. , Zheng,Y.S., Zhang, C. (2020). Analyzing failure of casing head slip hanger [J]. Engineering Failure Analysis,108,104301.https://doi.org/10.1016/j.engfailanal.2019.104301.

[6] Zhang Z., Sang,P.F., Sang,Z.P., Hou,D., Lv,Y.Y., Zheng,Y.S., Zhang, C. (2020). Study on failure mechanism and sealing performance optimization of compression packer[J] Engineering Failure Analysis,206,106176. https://doi.org/10.1016/j.engfailanal.2022.106176.

[7] C. K., T.,M., D. B.(2014). Fatigue cracks in railway bridge hangers due to wind induced vibrations – Failure analysis, measures and remaining service life estimation[J]. Engineering Failure Analysis,43,232–252. http://dx.doi.org/10.1016/j.engfailanal.2014.02.019.

[8] Liu,Y., Lian, Z.H., Shi,T.H., Sang,P.F.(2019). Fracture failure analysis and research on slip of casing head[J]. Engineering Failure Analysis, 97, 589–604. https://doi.org/10.1016/j.engfailanal.2019.01.058.

[9] Liu,Y., Lian,Z.H., (2021). Failure analysis on rubber sealing ring of mandrel hanger and improvement in extreme environments[J]. Engineering Failure Analysis,125,105433. https://doi.org/10.1016/j.engfailanal.2021.105433.

[10] Liu,Y., Qian,L.Q., Xia,C.Y. Zou,J.Y, Yi,X.Z.(2023). Failure analysis and structural optimization of rubber core and support rib of full-size ball blowout preventer[J] Engineering Failure Analysis,143,106865.https://doi.org/10.1016/j.engfailanal.2022.106865.

[11] Liu,Y.,She, Y.Z., Li,W.Q. (2025). Research on Working Mechanism and Structural Optimization of High-Speed Bearing of Tricone Bits Based on Finite Difference Method[J]. Journal of Tribology,147(4) :044103-1.https://doi.10.1115/1.4066946.

[12] Janardhan, R. S., Amjad, K., Manoj S., Nasser, B., Talal, N.. (2021). Implications of failure of alloy 718 (UNS N07718) tubing hanger in sour well[J].

Engineering Failure Analysis,120,105060. https://doi.org/10.1016/j.engfailanal.2020.105060.

[13] Chen, Y., Xiao G.P., Yi,H., Ding,Y., Tan.,J.J. (2022). Investigation on critical load and sealing capacity of mandrel hanger wellhead[J]. International Journal of Pressure Vessels and Piping,199,104767. https://doi.org/10.1016/j.ijpvp.2022.104767.

[14] Zeng,J., Xie,W.W., Kou,B.B., Lu,J.A, Li,X.C., Cai,D.J., Shi,H.X., Zhang, K.W., Liu,H.Q., Li,J., Li,B. (2023). Lateral bearing characteristics of subsea wellhead assembly in the hydrate trial production engineering[J]. China Geology,6 ,455−465. https://doi.org/10.31035/cg2022057.

[15] Xiang, S.L., Zhang, Z., Xu, H.L., Hu, S.C., Sang, P.F., Zhao, Y.J., Ding, J., Peng, N. (2025). Investigation on Complex Nonlinear Flow-induced Vibration Characteristics of Production Strings in Ultra-deep Gas Wells[J]. Applied Mathematical Modelling,146,116156. https://doi.org/10.1016/j.apm.2025.116156.

[16] Harshkumar, P., Saeed, S., Catalin, T., Ramadan, A. (2019). Performance evaluation and parametric study of elastomer seal in conventional hanger assembly[J]. Journal of Petroleum Science and Engineering,175,246–254. https://doi.org/10.1016/j.petrol.2018.12.051.

[17] Harshkumar, P., Saeed, S., Ramadan, A., Catalin, T. (2019). Review of elastomer seal assemblies in oil & gas wells: Performance evaluation, failure mechanisms, and gaps in industry standards[J]. Journal of Petroleum Science and Engineering,179,1046–1062. https://doi.org/10.1016/j.petrol.2019.05.019.

[18] Shawgi, A., Saeed, S., Chinedum, E. (2020). Review of gas migration and wellbore leakage in liner hanger dual barrier system: Challenges and implications for industry[J]. Journal of Natural Gas Science and Engineering ,78 ,103284. https://doi.org/10.1016/j.jngse.2020.103284.

[19] Pablo, C., Jose, L. O., Alberto, A., Guillermo, C. (2019). Undetected non-conformities in material processing led to a service failure in a casing hanger during pre-fracture operation[J]. Engineering Failure Analysis,104,203–215. https://doi.org/10.1016/j.engfailanal.2019.05.026

[20] Charlton, O.S., Jose, R.M. S., Gilberto, B. E. (2020). Wellhead axial movements in subsea wells with partially cemented surface casings[J]. Journal of Petroleum Science and Engineering,194,107537. https://doi.org/10.1016/j.petrol.2020.107537.